



A Random Matrix Theory Approach to National Procurement Spending

Applications to the CC130 Hercules Fleet Performance

David W. Maybury
Materiel Group Operational Research

DRDC CORA TM 2010-168
August 2010

Defence R&D Canada
Centre for Operational Research and Analysis

Materiel Group Operational Research
Assistant Deputy Minister (Materiel)



National
Defence

Défense
nationale

Canada

A Random Matrix Theory Approach to National Procurement Spending

Applications to the CC130 Hercules Fleet Performance

David W. Maybury

Materiel Group Operational Research

Defence R&D Canada – CORA

Technical Memorandum

DRDC CORA TM 2010-168

August 2010

Principal Author

Original signed by David W. Maybury

David W. Maybury

Approved by

Original signed by R.M.H. Burton

R.M.H. Burton
Acting Section Head (Joint and Common OR)

Approved for release by

Original signed by D.S. Haslip

D.S. Haslip
Acting Chief Scientist

- © Her Majesty the Queen in Right of Canada as represented by the Minister of National Defence, 2010
- © Sa Majesté la Reine (en droit du Canada), telle que représentée par le ministre de la Défense nationale, 2010

Abstract

We apply the methods of random matrix theory to search for relationships between National Procurement spending and the performance of the CC130 fleet. By understanding the eigenvalue spectrum of correlation matrices connected to performance and spending, we construct the minimal spanning tree of the system to identify networked hierarchies in the data. We find that no meaningful relationship exists between spending and high level performance indicators, suggesting that the fleet responds to spending shocks in an inelastic manner. The results indicate that the CC130 fleet is maintained robustly and that funding has not fallen below a critical level that would induce correlations between spending and performance. The techniques we apply in this study can be applied generally to any project that requires an understanding of correlations in data.

Résumé

Nous appliquons les méthodes de la théorie des matrices aléatoires pour découvrir comment les dépenses d'approvisionnement national et le rendement de la flotte de CC130 sont interreliés. En comprenant le spectre des valeurs propres des matrices de corrélations se rapportant au rendement et aux dépenses, nous construisons l'arbre maximal minimal du système dans le but de cerner les hiérarchies intriquées dans les données. Nous découvrons qu'il n'existe pas de lien significatif entre les dépenses et les indicateurs de rendement de haut niveau, ce qui donne à penser que la flotte a une réaction inélastique aux chocs de dépenses. Ces résultats révèlent que l'entretien de la flotte des CC130 est robuste et que le financement n'est pas tombé sous le seuil critique qui se traduirait par des corrélations entre les dépenses et le rendement. Les mêmes techniques peuvent être appliquées à n'importe quel projet pour lequel il faut comprendre les corrélations entre les données.

This page intentionally left blank.

Executive summary

A Random Matrix Theory Approach to National Procurement Spending

David W. Maybury; DRDC CORA TM 2010-168; Defence R&D Canada – CORA; August 2010.

Over the last seven years, ADM(Mat) has sought a deeper understanding of the relationship between National Procurement (NP) spending and fleet performance in the hopes that such linkages would provide a first step in the development of a funding optimization procedure. Furthermore, an understanding of spending effects on fleet operations might also provide insight into optimal sparing levels, optimal maintenance activities and schedules, and optimal replacement times. In this study we take an approach different from past studies that attempted to uncover relationships in fleet performance and spending. We apply results from random matrix theory and graph theory to search for relationships in the data. To demonstrate the methods, we focus our study on the CC130 fleet, using ten years of data, as requested by the DCOS(Mat).

We demonstrate that excess noise in the correlation measures between CC130 performance indicators represents a serious obstacle in developing a model that would connect NP spending to fleet performance. Our results demonstrate that NP spending does not have a strong relationship with performance. Since NP spending connects to the larger economy, fluctuations in costs associated with the CC130 fleet can quickly divorce from underlying financials. The excess noise in the correlation measures tells us that randomness plays a large role in any apparent correlation between NP spending and performance indicators. Changes in NP spending at the levels observed in the data have little impact on performance. We can conclude that maintenance activity is highly robust – spending shocks of the size observed in the data do not have a statistical impact on major performance indicators. Thus, given the funding levels over the last ten years, the CC130 fleet does not respond to spending fluctuations. The methods we use in this paper can be applied to other fleets and equipment. In addition to searching for relationships between spending and performance, we can apply the theory of random matrices to other instances in which we need to examine correlations in data.

Sommaire

A Random Matrix Theory Approach to National Procurement Spending

David W. Maybury ; DRDC CORA TM 2010-168 ; R & D pour la défense Canada – CARO ; août 2010.

Au cours des sept dernières années, le SMA(Mat) a voulu mieux comprendre les liens entre les dépenses d'approvisionnement national (AN) et le rendement de la flotte, dans l'espoir que ces liens marquent le point de départ de l'élaboration d'une procédure d'optimisation du financement. En outre, le fait de comprendre les effets que les dépenses ont sur la flotte pourrait aider à définir les quantités optimales de pièces de rechange à garder en stock, les activités et les calendriers d'entretien optimaux ainsi que les meilleurs calendriers de remplacement. Dans la présente étude, nous n'avons pas adopté l'approche utilisée dans les études antérieures qui avaient pour objet de cerner les liens entre les dépenses et le rendement de la flotte. Nous appliquons les résultats obtenus à l'aide de la théorie des matrices aléatoires et de la théorie des graphes afin de chercher les liens entre les données. Pour démontrer les méthodes, nous avons choisi d'examiner la flotte de CC130 dans la présente étude et utilisé les données sur dix ans, à la demande du SCEM(Mat). Nous démontrons que la présence de bruit excessif dans les mesures des corrélations entre les indicateurs de rendement de la flotte des CC130 entrave considérablement l'élaboration d'un modèle qui établirait les liens entre les dépenses d'AN et le rendement de la flotte. Nos résultats montrent l'absence de lien fort entre les dépenses d'AN et le rendement. Comme les dépenses d'AN sont liées à l'économie dans son ensemble, les fluctuations de coût associées à la flotte de CC130 peuvent rapidement se séparer des données financières sous jacentes. La présence de bruit excessif dans les mesures des corrélations révèle que le caractère aléatoire compte pour beaucoup dans toute corrélation apparente entre les dépenses d'AN et les indicateurs de rendement. Les variations des dépenses d'AN de l'ordre de celles qui sont observées dans les données ont peu d'effet sur le rendement. Nous pouvons conclure que l'entretien est très robuste ; les chocs de dépenses de la taille de ceux qui sont observés dans les données n'ont pas d'impact statistique sur les principaux indicateurs de rendement. Par conséquent, étant donné les niveaux de financement des dix dernières années, la flotte de CC130 ne réagit pas aux fluctuations des dépenses. Les méthodes que nous utilisons dans la présente étude peuvent aussi s'appliquer à d'autres flottes et équipements. Nous pouvons utiliser la théorie des matrices aléatoires non seulement pour découvrir les liens entre les dépenses et le rendement, mais aussi dans d'autres cas, lorsqu'il s'agit d'examiner les corrélations qui existent entre les données.

Table of contents

Abstract	i
Résumé	i
Executive summary	iii
Sommaire	iv
Table of contents	v
List of figures	vii
Acknowledgements	ix
1 Introduction	1
1.1 Background	1
1.2 Scope	3
2 Methodology	4
2.1 Correlations and random matrix theory	5
2.2 Minimal spanning tree and clustering	9
3 Results	12
3.1 Data selection	12
3.2 Analysis	13
3.3 Total NP analysis with synchronous time series	14
3.4 Total NP analysis with time lags time	16
3.5 Spares and R&O analysis with synchronous time series	17
3.6 Spares and R&O analysis with time lags	17
4 Conclusions	20
References	24
Annex A: Random matrix theory primer	25

Annex B: Fleet indicator definitions 29

List of Acronyms 34

List of figures

Figure 1:	Empirically measured correlations among 20 uncorrelated time series each with 30 measurements. Note the large number of significant spurious cross correlations (off diagonal elements).	5
Figure 2:	Empirically measured correlations among 20 uncorrelated time series each with 300 measurements. Notice that the spurious cross correlations (off diagonal elements) diminish relative to figure 1.	6
Figure 3:	Empirical eigenvalue spectrum of the time series correlation matrix given by figure 1 with the theoretical curve predicted by random matrix theory. Up to finite size effects, the data is explained by the theoretical curve.	9
Figure 4:	Dendrogram on the ultrametric space for the data considered in the matrix eq.(16). Note that, at the 70% of the maximum of the ultrametric space level, the dendrogram singles out two clusters from the data.	11
Figure 5:	The empirical eigenvalue spectrum (histogram) for total NP spending synchronously matched to performance indicators. The theoretical curve for $Q = 119/14$ infinite random matrix is superimposed.	15
Figure 6:	Dendrogram for NP spending (time series 14) synchronously matched to performance indicators. Notice that NP spending branches early in the dendrogram indicating that NP spending lies far from the performance indicators in the ultrametric space. The number labelling for each time series is the same as that given in the text.	16
Figure 7:	Eigenvalue spectrum of performance indicators with lagged NP spending with theoretical curve (a) lag 1 month, (b) lag 3 months, (b) lag 6 months, and (b) lag 12 months.	18
Figure 8:	Dendrogram of performance indicators with lagged NP spending (a) lag 1 month, (b) lag 3 months, (b) lag 6 months, and (b) lag 12 months. Note that NP spending (time series 14) branches early in each dendrogram indicating that NP spending does not form a hub within the MST.	19
Figure 9:	(a) Eigenvalue spectrum with spares and R&O spending synchronously matched with theoretical curve. (b) Dendrogram for the performance indicators with synchronously matched spares and R&O spending (time series 14 and 15).	20

Figure 10: Eigenvalue spectrum of performance indicators with lagged spares and R&O spending with theoretical curve (a) lag 1 month, (b) lag 3 months, (b) lag 6 months, and (b) lag 12 months. 21

Figure 11: Dendrogram of performance indicators with lagged NP spending (a) lag 1 month, (b) lag 3 months, (b) lag 6 months, and (b) lag 12 months. Note that spares and R&O spending (time series 14 and 15) branch early in each dendrogram indicating that pares and R&O spending do not for a hub within the MST. 22

Figure A.1: Eigenvalue spectra for infinite random matrices with $Q = 1$, $Q = 2$, $Q = 5$. Note the presence of λ_{\min} and λ_{\max} in each case. 27

Acknowledgements

I would like to thank Dr. Paul E. Desmier (DMGOR) for his help in securing FMAS data for this study and for his help with understanding the in-house history of past work on this topic. I have also greatly benefited from discussions with Mr. David Shaw, former head of Acquisition Support Team (DMGOR).

This page intentionally left blank.

1 Introduction

Things are seldom what they seem.

Skim milk masquerades as cream.

— Gilbert and Sullivan, H.M.S. Pinafore

1.1 Background

Over the last seven years, ADM(Mat) has sought a deeper understanding of the relationship between National Procurement (NP) spending and fleet performance. The discovery of linkages between spending and operational availability (A_o) would provide a first step in the development of a funding optimization procedure. ADM(Mat) desires a tool based on NP spending/performance relationships that would help elicit the best possible fleet and equipment performance at the best possible cost. Furthermore, an understanding of spending effects on fleet operations might also provide insight into optimal sparing levels, optimal maintenance activities and schedules, and optimal replacement times. In a period of declining budgets, ADM(Mat) requires an analysis of the impact NP spending has on DND fleets.

While the problem seems well posed, any potential analysis that attempts to isolate the effect of spending levels on fleet performance faces extreme hurdles. We immediately recognize that since spending connects to a myriad of exogenous economic factors, such as inflation, price fluctuations in materiel, and worldwide supply chain pressures, a simple one-to-one map cannot exist between spending and any performance measure. For example, in any one period, spending may rise as the result of an increase in the cost of lubricants while performance may decline due to the discovery of an unexpected aging effect. The problem of connecting NP spending to fleet performance must rely on a statistical analysis of changes in both fleet indicators and costs as primary inputs.

The last five years has seen periods of concentrated efforts by the Directorate of Materiel Group Operational Research (DMGOR) to uncover relationships between NP spending and fleet performance. Initially, the DMGOR followed two promising methods to find linkages in the NP costing data and fleet performance indicator data with the eventual goal of creating the “Providing a New Assessment for Costing Equipment Availability” model (PANACEA) [1]. The first method treats operational availability as the steady state solution of a differential equation that contains a characteristic relaxation time. In this toy model, A_o tracks a mean reverting process – A_o relaxes back to its equilibrium level after a shock disturbs the system. The model contains qualitative features that have direct interpretations through performance indicators (such as mean time between failures, mean down times, and response parameters) which afford an asymptotic solution in terms of twelve free parameters. With the use of suitable approximations and redefinitions, the large free parameter set can be reduced to five inputs. The second attempted solution

uses feedforward artificial neural networks to search for a functional relationship between funding and A_o for the CP140, the CH124, the CC130, and the CF188.

In effect, both previous attempts use a filter method that recursively makes predictions while updating internal system parameters at each time step in the presence of noise. The system variables that both models attempt to isolate act as elasticity parameters for NP spending with performance¹. Since the data contains noise, the filter techniques rely on stochastic methods to update estimates of the response parameters, thereby updating the estimate of the elasticity of NP spending on performance. The most celebrated filter used in stochastic control is the Kalman filter (for example, see [2], and [3]), which requires an understanding of the noise and covariances within the system. The previous two models have broad similarities with Kalman filters and thus we understand the origin of each model's response parameters along with their estimates, which carry information about correlations within the fleet's time series data.

Unfortunately, both models have failed to answer the question as to whether a relationship exists in the data. The mean reverting differential equation contains too many free parameters given the summary level nature of the data and the data's intrinsic noise. The artificial neural network could not be trained at a sufficient level to find meaningful relationships. In fairness to the models and the hard work that went into the attempts, looking for a map between fleet performance and summary level data hinges on approximations. Each of the approximations within the models, while in themselves reasonable, do not capture enough of the complexity of a fleet. Embedded within the fleet's operations are multiple queues – from sparing to scheduled inspections – that interact in highly non-trivial ways. On the other hand, an attempt to capture the entire fleet's operations bottom up and connect the entire problem to funding would not only prove exceedingly difficult, but it is not clear that such an undertaking would provide insight into funding relationships². In the end, such a model might prove more descriptive than predictive.

This paper will take a different tack relative to past approaches. Instead of attempting to build complicated analytical relationships between performance indicators and funding, we search the data for basic information content. Given that the filter method approaches of previous attempts implicitly require an understanding of covariances, we focus our efforts on the correlation structure of the data. The limit of the information content within the

¹Elasticity is a concept from economics. The price elasticity of demand is defined as $e = \frac{\Delta Q/Q}{\Delta P/P}$ where Q and P denote demand and price respectively. Elasticity measures the effect of relative changes between parameters.

²While a detailed bottom up stochastic queuing model built around filter methods might identify potential opportunities to increase efficiency by isolating bottlenecks in the fleet's combined sparing policy, maintenance and training schedules, and other performance driven activities, such a study would require huge amounts of data and a tremendous amount of concentrated effort by a team of analysts. Given the complicated nature of several interacting queues, any attempt at removing a bottleneck to increase efficiency may lead to new unanticipated bottlenecks in other parts of the system. It is not obvious that a detailed study of low level data would provide sufficient value above existing tools.

data will establish the level of connections that we can make within the fleet and address the question as to whether it makes sense to embark on constructing a detailed model. We adopt an agnostic philosophy about which relationships should have strong links – we simply let the data direct us. The methods that we employ borrow heavily from quantitative finance. In particular, we apply the same techniques that quantitative analysts use to search for stock hierarchies and networks within the market. Our problem of searching for links between fleet performance indicators and funding parallels the portfolio problem of identifying market sectors for optimal capital allocation. By applying these methods, we can identify the hubs and clusters in performance and costing networks (or the lack thereof). The number, size, and strength of the clusters in the data will determine the information content and therefore help resolve the general applicability of filter methods with NP spending and performance data. Given the new approach taken in this paper, we focus on the methodology by using one DND fleet, the CC130, as a template for the application.

1.2 Scope

ADM(Mat) requires a study to identify exploitable information from the relationships between NP spending and fleet performance to optimize NP allocations. In particular, a former COS(Mat) [4] and the current DCOS(Mat) have tasked the DMGOR to develop a model or approach that will allow a more logical articulation of the linkage between the resources allocated to National Procurement in the areas of spares, repair and overhaul (R&O), and other integrated logistics support (ILS) activities. In discussions with the DCOS(Mat), the CC130 Hercules lift fleet was identified as a priority for this study. The DMGOR's response to this request focuses on discovering information by isolating clusters in NP spending and performance data with the CC130 fleet. Our modelling methods aim to:

- use the theory of random matrices to understand correlations within time series data;
- identify clusters in the correlation data through the use of graph theory techniques; and
- establish the feasibility of continuing future studies seeking to create an NP spending optimization model.

We obtained all performance data on the CC130 from the AEPM PERFORMA database [5] and NP data from Financial and Managerial Accounting System (FMAS) [6].

We organize the paper in three parts. Following the introduction we explain the modelling techniques in section 2. In section 3, we examine the data and display key results from the analysis. Finally, section 4 contains the conclusions and discusses future avenues for research. We reserve the annexes for a detailed treatment of the mathematical techniques and technical definitions.

2 Methodology

To determine the influence of NP spending on fleet performance we need to examine how changes in spending and performance measures correlate. Recall that the correlation coefficient (for example, see [7]) between two random variables is defined by³

$$\rho(X, Y) = \frac{E[(X - \hat{x})(Y - \hat{y})]}{\sigma(X)\sigma(Y)} \quad (1)$$

where \hat{x} and \hat{y} respectively denote the mean of the random variables X and Y , and $\sigma(\cdot)$ denotes the standard deviation. The correlation coefficient has the range $[-1, 1]$ for any pair of random variables. Perfectly correlated (anti-correlated) random variables have $\rho = +(-)1$. If two random variables are highly correlated, we will find that changes in one random variable match the changes in the other.

Searching for relationships in time series data requires an understanding of cross correlations. In particular, the relationship between incremental changes in time series data can help us reveal information content in the data. Thus, to discover relationships, it appears we need only to estimate the correlation coefficient between time series and isolate only those measurements that have a correlation coefficient above a predetermined cutoff (e.g. $|\rho| = 0.7$). Unfortunately, this simple approach can lead to disaster – spurious correlations⁴ spoil our ability to resolve information, especially if the data contains a high level of noise.

As a concrete example, imagine that we have 20 time series constructed as uncorrelated, *i.i.d.*⁵ Gaussian noise with zero mean and unit variance. Given enough measurements, our estimates for each cross correlation coefficient will tend to zero. Unfortunately, this trend toward zero often requires large amounts of data to become apparent. Let us assume that our 20 independent time series each have 30 measurements and let us construct the correlation matrix from simulated data. By construction, each time series is uncorrelated yet the values of the correlation matrix displayed in figure 1 show evidence of substantial cross correlations. If we were to use the numerical estimates of the cross correlations given in figure 1 as model inputs for cross correlations, we would be led horribly astray. A priori we know that no relationships exist in the data, but the correlation matrix with only

³The operator $E(\cdot)$ denotes the expectation.

⁴Roughly speaking, a spurious correlation is a relationship that occurs by chance with no underlying connection. Spurious correlations frequently appear in the popular media and perhaps the most fantastic example is the Super Bowl Indicator for the stock market. This indicator claims that if the National Football Conference wins the super bowl, then the Dow Jones Industrial Average will see a bull market over the coming year whereas a win by the American Football Conference will see a bear market. The Super Bowl Indicator has a success rate of approximately 80% over the last 40 years. This result stems purely from coincidence yet the data appears to have a high level of correlation. When we have a large amount of data, spurious correlations – like the Super Bowl Indicator – will frequently appear and we must guard ourselves from incorrect conclusions. (Lest our retirement invest strategy revolves around the performance of the NFL!)

⁵*i.i.d.* stands for independent and identically distributed.

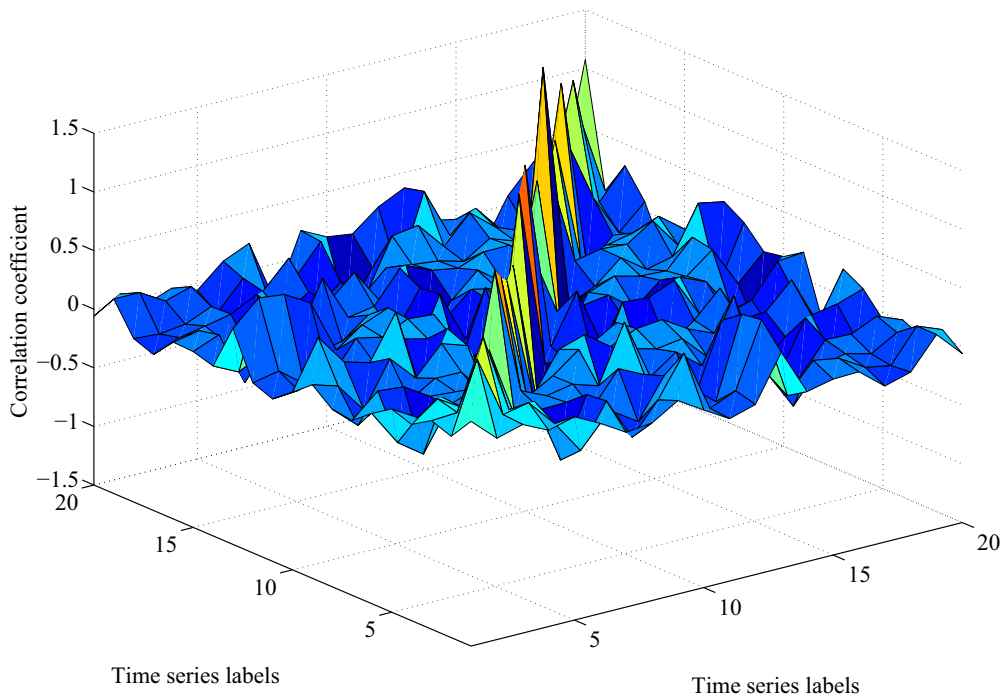


Figure 1: Empirically measured correlations among 20 uncorrelated time series each with 30 measurements. Note the large number of significant spurious cross correlations (off diagonal elements).

30 measurements across 20 time series contains many spurious correlations. On the other hand, if we use the same 20 time series but with an order of magnitude more measurements, as displayed in figure 2, we see that the spurious correlations greatly diminish.

Searching for cross correlations in data proves a difficult challenge. The appearance of spurious correlations interferes with our ability to separate bona fide information from random fluctuations. In general, correlation matrices obtained from real data come with a mask, called noise dressing [8], that impedes our ability to understand relationships. We require an understanding of the noise dressing that sits on top of the actual correlation matrix to make progress in identifying information.

2.1 Correlations and random matrix theory

The problem of noise dressing with correlation matrices occurs in many fields – from nuclear physics to financial mathematics – and the theory of random matrices [9], [10], [11]

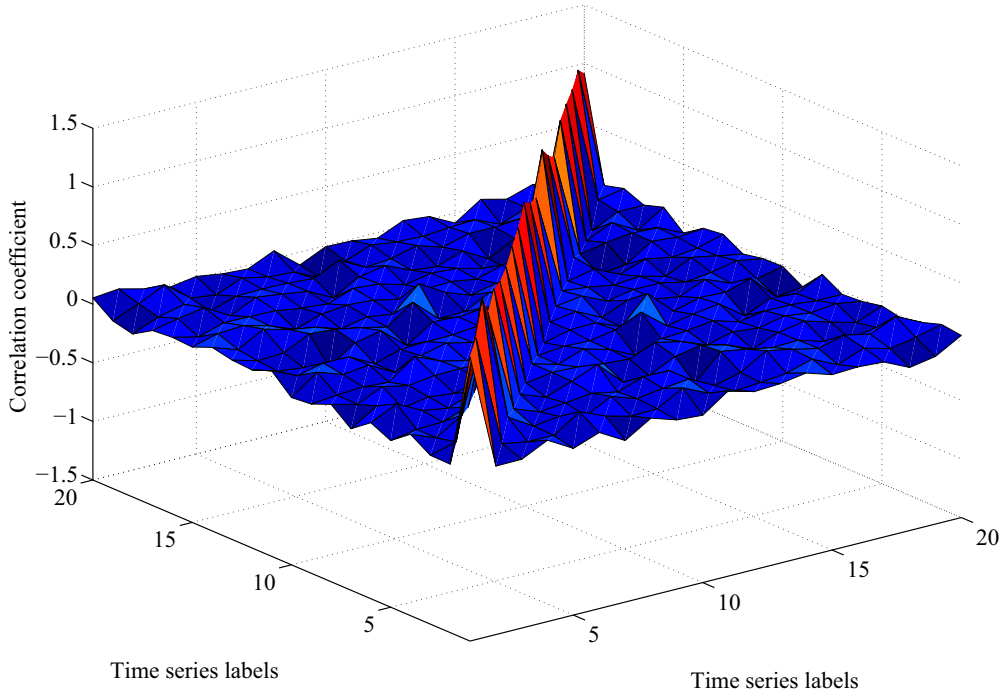


Figure 2: Empirically measured correlations among 20 uncorrelated time series each with 300 measurements. Notice that the spurious cross correlations (off diagonal elements) diminish relative to figure 1.

forms a pillar in understanding the limits of data. To introduce the application of random matrices to the NP spending and the CC130 fleet performance problem, consider a set of time series which contain known correlated sectors. Let $\xi_i(t)$ denote the i -th time series, where $t \in 1, 2, 3, \dots, T$ labels each measurement. Normalizing each time series by transforming the data to standard form,

$$\sum_{t=1}^T \frac{\xi_i(t)}{T} = 0, \quad \sum_{t=1}^T \frac{\xi_i(t)^2}{T} = 1, \quad \forall i \quad (2)$$

we find that the correlation matrix becomes

$$C_{ij} = \frac{1}{T} \sum_{t=1}^T \xi_i(t) \xi_j(t). \quad (3)$$

Given that we have explicitly assumed the existence of correlated sectors, we can write each time series as [8]

$$\xi_i(t) = \frac{\sqrt{g_{s_i}} \eta_{s_i}(t) + \varepsilon_i(t)}{\sqrt{1 + g_{s_i}}}, \quad (4)$$

where $g_{s_i} > 0$ (and sets the strength of the correlations), the s_i are integers denoting each sector, and $\eta_{s_i}(t)$ and $\varepsilon_i(t)$ are uncorrelated *i.i.d.* Gaussian noise terms. We see that as $T \rightarrow \infty$ the correlation matrix becomes block diagonal, namely

$$C_{ij} = \frac{g_{s_i} \delta_{s_i, s_j} + \delta_{i,j}}{1 + g_{s_i}}, \quad (5)$$

where δ_{ij} denotes the usual Kronecker delta. The block diagonal structure of C_{ij} reveals a simple pattern for the eigenvalues. For each block n_s we find one eigenvalue

$$\lambda_{s,0} = \frac{1 + g_s n_s}{1 + g_s}, \quad (6)$$

and $n_s - 1$ degenerate eigenvalues

$$\lambda_{s,1} = \frac{1}{1 + g_s}. \quad (7)$$

The eigenvalue spectrum of C_{ij} give us a clue on the way in which correlated sectors emerge from the data. We can identify large correlated sectors with large eigenvalues (*i.e.* $n_s \gg 1$). On the other hand, we see that small eigenvalues can arise from both small and large sectors that exhibit strong correlations. Thus an excess of large and small eigenvectors can help us locate large and small correlated sectors. In particular, a large excess of small eigenvalues suggests the presence of many small sectors with strong correlations⁶.

While the analysis of the block diagonal structure of C_{ij} yields a qualitative identification procedure, we need a more concrete framework to understand the spectrum of the eigenvalues. We see that each block in the idealized correlation matrix contains one large eigenvalue and $n_s - 1$ degenerate eigenvalues, but random noise in the correlation matrix will split degeneracies and alter the position of all the eigenvalues. Understanding the noise dressing in the correlation matrix represents a critical path item for extracting information.

The central limit theorem applied to random matrices sheds light on our problem [10]. The eigenvalue distribution of large random matrices has a calculable expression. Thus, knowing the statistical properties of the elements of a random matrix, we can compute the corresponding eigenvalue spectrum. Once we obtain the underlying spectrum associated with a random matrix, we can compare the result to the spectrum obtained from empirical data. Distortions in the empirical eigenvalue spectrum relative to a random matrix signal the presence of correlated sectors. To calculate the eigenvalue spectrum of a random matrix, suppose that we have an $M \times M$ real symmetric matrix, \mathbf{C} . The matrix \mathbf{C} will have real

⁶The block diagonal structure of the discussion assumes positive correlations between time series. The observations can be generalized to included negative correlations with the introduction of spin variables $\sigma_i = \pm 1$ in eq.(4). These changes do not affect the qualitative arguments in the discussion. For more details see [8].

eigenvalues λ_a , $a = 1, 2, 3, \dots, M$. We can write the density of eigenvalues as,

$$\rho(\lambda) = \frac{1}{M} \sum_{a=1}^M \delta(\lambda - \lambda_a), \quad (8)$$

where δ denotes the Dirac delta function. We now define the resolvent of the \mathbf{C} as,

$$\mathbf{G}(\lambda) = \left(\frac{1}{\mathbf{I}\lambda - \mathbf{C}} \right), \quad (9)$$

where \mathbf{I} denotes the $M \times M$ identity matrix. Using well known results from linear algebra, we can rewrite the trace over $\mathbf{G}(\lambda)$ in terms of the eigenvalues of \mathbf{C} , namely

$$\text{Tr} \mathbf{G}(\lambda) = \sum_{a=1}^M \frac{1}{\lambda - \lambda_a}. \quad (10)$$

In the large M limit, we can use the identity (see Annex A for proof)

$$\frac{1}{x - i\varepsilon} = \text{PP} \frac{1}{x} + i\pi\delta(x) \quad (\varepsilon \rightarrow 0), \quad (11)$$

where PP denotes the principal part, to write the density function as

$$\rho(\lambda) = \lim_{\varepsilon \rightarrow 0} \frac{1}{M\pi} \text{Im}(\text{Tr} \mathbf{G}(\lambda - i\varepsilon)). \quad (12)$$

The integral representation of the determinant of real symmetric matrices (see Annex A) allows us to compute $\mathbf{G}(\lambda)$ in a tractable form. If we assume that $\mathbf{C} = \mathbf{H}\mathbf{H}^T$, where \mathbf{H} is an $M \times N$ matrix composed of *i.i.d.* Gaussian elements with zero mean and variance σ^2/N , we find that the eigenvalue spectrum of \mathbf{C} becomes

$$\rho(\lambda) = \frac{\sqrt{4\sigma^2 Q\lambda - (\sigma^2(1-Q) + Q\lambda)^2}}{2\pi\lambda\sigma^2}, \quad (13)$$

where $M \rightarrow \infty$, $N \rightarrow \infty$ such that $M/N = Q \geq 1$. Notice that the eigenvalue spectrum of eq.(13) contains λ_{\min} and λ_{\max} dictated by the real domain of the radical.

To illustrate the application of random matrices to time series data, let us return to our example in which we examined the correlation matrix for 20 time series with 30 measurements. Recall that the resulting correlation matrix revealed many large spurious correlations (see figure 1). Given the time series data set, we can compare the empirical eigenvalue spectrum of the correlation matrix to the spectrum of an infinite random correlation matrix with $Q = 3/2$. In figure 3, we display the empirical eigenvalue spectrum from the random time series as a histogram along with the theoretical eigenvalue spectrum of the random correlation matrix. Notice that the theoretical curve fully explains the histogram which suggests that all correlations exhibited by the empirical correlation matrix are spurious.

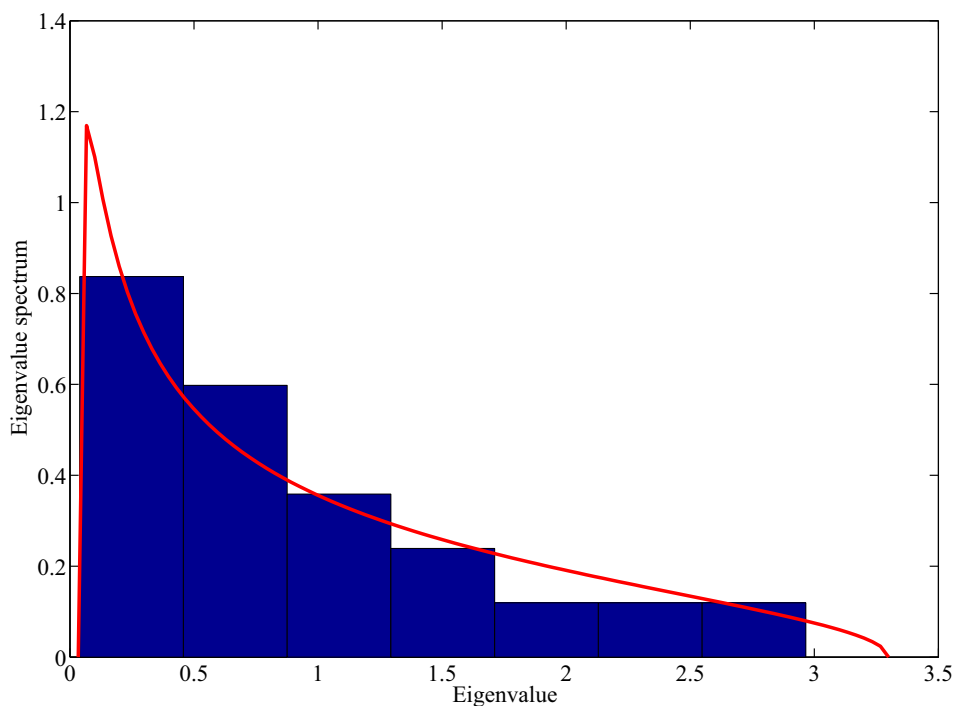


Figure 3: Empirical eigenvalue spectrum of the time series correlation matrix given by figure 1 with the theoretical curve predicted by random matrix theory. Up to finite size effects, the data is explained by the theoretical curve.

2.2 Minimal spanning tree and clustering

The theory of random matrices helps us determine the presence of correlated sectors in the data. If we find that the spectrum of a correlation matrix does not concord with the spectrum obtained from a random matrix, then we have evidence for correlated clusters. While random matrix theory helps us recognize the existence of a correlation structure, the eigenvalue spectrum does not directly tell us the number of clusters in the data nor which set of time series form a cluster. To identify clusters, we will use the stock market and condensed matter physics as inspiration. Methods in graph theory can help identify networks and hierarchies in clustered data [12]. In particular, the application of graph theoretic techniques [13] to stock markets have not only helped identify market sectors, but have also imparted a deeper understanding of the entire economic organization of financial markets.

To begin our application of graph theory methods to our problem, we need the concept of distance among correlated time series, *i.e.* we need a metric space. It can be shown [13]

that

$$d_{ij} = \sqrt{2(1 - \rho_{ij})} \quad (14)$$

satisfies the requirements of a Euclidean distance where ρ_{ij} denotes the correlation coefficient between the i -th and j -th time series (see eq.(1)). While we can use eq.(14) to compute the distance between any pair of time series, we cannot directly use the distance to isolate sectors. Noise dressing interferes with a clean interpretation of the distance between pairs of time series.

We can overcome the shortcomings of the Euclidean distance by placing the time series on an ultrametric space. In an ultrametric space, the triangle inequality of a metric space is replaced by the stronger condition (called the ultrametric inequality)

$$d_{ij} \leq \max[d_{ik}, d_{kj}]. \quad (15)$$

It turns out that given a metric distance with n objects, many ultrametric spaces can be constructed through re-partitioning (see [13] and references therein). Of all the ultrametric spaces that can be associated with a distance d_{ij} , the subdominant ultrametric space singles itself out as it can be obtained from the minimal spanning tree (MST) that connects the n objects. The MST of a weighted graph is a tree with $n - 1$ edges that minimizes the sum of the edge distances. In the end, subdominant ultrametric space yields a unique indexed hierarchy for our problem. Fortunately a simple algorithm exists – the Kruskal algorithm (see [13] and references therein) – which allows us to directly construct the MST with a Euclidean distance.

As an illustration of the Kruskal algorithm, consider the Euclidean distance matrix obtained from a hypothetical correlation matrix:

$$\begin{pmatrix} & \mathbf{A} & \mathbf{B} & \mathbf{C} & \mathbf{D} & \mathbf{E} & \mathbf{F} \\ \mathbf{A} & 0 & 0.4700 & 0.8900 & 1.2000 & 0.9800 & 1.1100 \\ \mathbf{B} & 0.4700 & 0 & 1.0100 & 0.2000 & 0.8900 & 1.3000 \\ \mathbf{C} & 0.8900 & 1.0100 & 0 & 0.7500 & 0.5200 & 1.1800 \\ \mathbf{D} & 1.2000 & 0.2000 & 0.7500 & 0 & 0.9900 & 0.7100 \\ \mathbf{E} & 0.9800 & 0.8900 & 0.5200 & 0.9900 & 0 & 0.4400 \\ \mathbf{F} & 1.1100 & 1.3000 & 1.1800 & 0.7100 & 0.4400 & 0 \end{pmatrix}. \quad (16)$$

Applying the Kruskal algorithm, we need to parse through the distance matrix proceeding pair-wise from the closest pair to the farthest. In our example B and D forms the closest pair with distance 0.20 and the next closest pair is E and F with distance 0.44. At this point we have two disjoint sections of the MST. We can see these two pairs represented by a dendrogram in figure 4. Notice that the height of the each pair in the dendrogram corresponds to each pair's Euclidean distance. We find that the next most closely connected pair is A and B with distance 0.47. In the ultrametric space, the A - B pair links A and D with

the same distance as A to B since B is already connected to D in the tree. We see the linkage in figure 4: A connects to the existing $B-D$ pair. Thus, ultrametrically, A is the same distance from B and D , with the largest Euclidean distance setting the ultrametric distance for the two pairs. Continuing through the distance matrix, we find the next closest pair is C and E (distance 0.52), which connects to F in the tree. Again, we see this linkage connects an existing pair, namely, the $E-F$ pair. Finally, the next connection, D and F with distance 0.71, completes the tree. If we continue parsing through the distance matrix, we encounter pairs that have already been fixed in the ultrametric space. For example, after the $D-F$ connection we have C and D with Euclidean distance of 0.75, but C and D are already connected in the tree and so we ignore this connection. We display the final ultrametric distance graph using the full dendrogram in figure 4. The colours of figure 4 show clusters

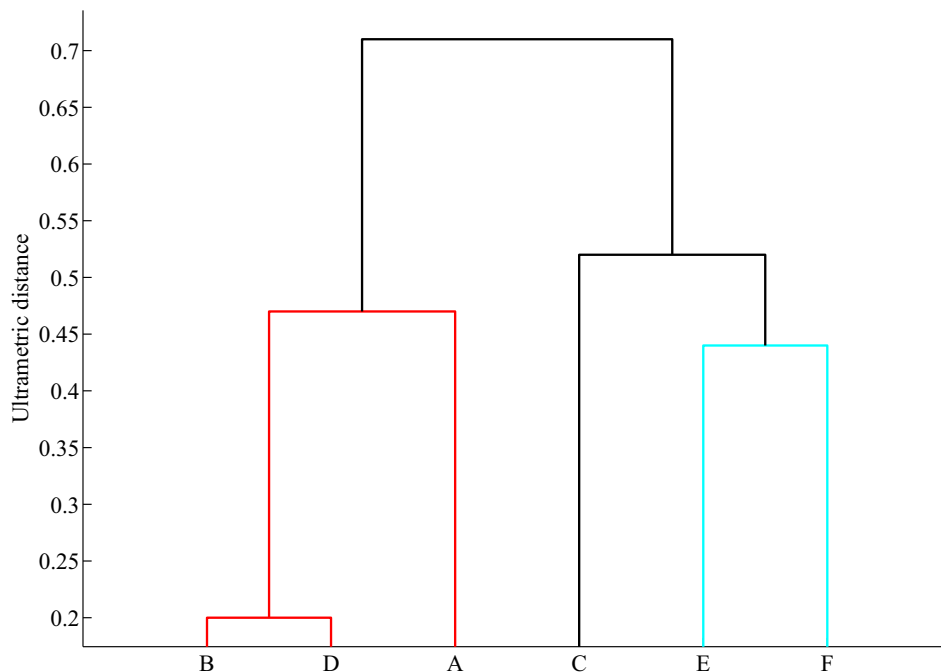


Figure 4: Dendrogram on the ultrametric space for the data considered in the matrix eq.(16). Note that, at the 70% of the maximum of the ultrametric space level, the dendrogram singles out two clusters from the data.

that have an ultrametric distance less than 70% of the maximal ultrametric distance in the tree. Thus, in our example, if we use 70% of the maximal ultrametric distance as a cutoff, we would conclude that $B-D-A$ and $E-F$ form independent data clusters. We will use this method to identify the presence of clusters in the NP spending and fleet performance data.

3 Results

3.1 Data selection

This study uses two data sources for the CC130 fleet: the PERFORMA database for fleet performance indicators and FMAS for NP spending levels. In total, we select 13 high level performance indicators that are expected to be significantly correlated with NP spending. Furthermore, we break down the NP spending into spares and R&O to help identify correlations within spending subsets. For this study, we use cost centres:

- 8485QA: CC130 Spares;
- 8485QB: T56 Engine Spares;
- 8485QH: CC130 Airframe Repair and Overhaul;
- 8485QJ: CC130 Miscellaneous Engine;
- 8485QL: CC130 T56 Engine Repair and Overhaul;
- 8485TM: Repair and Overhaul Flight Navigation Communication Equipment and;
- 8485UQ: CC130 Ties.

In the total NP part of the study, we used the data from all cost centres while in the R&O/spares breakdown part of the study we use 8485QA, 8485QB, 8485QH, and 8485QJ, 8485QL respectively.

Constraints imposed by the data limit the number of performance time series that we can use. In constructing a correlation matrix, we require the number of measurements to exceed the number of time series by approximately an order of magnitude to see a signal above the noise dressing. We use the PERFORMA database to extract 10 years of monthly data (December of 1998 to November 2008) for the performance indicators, thereby giving us 120 measurements. Thus, we must choose approximately 12 time series from the database. In the data selection process, we need to ensure that time series data captures the fleet's performance at a high level with an expectation that NP spending has an effect on the indicators themselves. The performance indicators we use are:

1. All failures
2. A_o – Overall operational availability
3. Corrective maintenance person-hours rate
4. First level A_o
5. Flying hours

6. Mean flying time between on aircraft corrective forms
7. Mean flying time between on aircraft preventive forms
8. Mean flying time between downing event
9. Off aircraft maintenance person-hour rate
10. On aircraft maintenance person-hour rate
11. On aircraft robs maintenance person-hour rate
12. Operation mission abort rate
13. Preventive maintenance person-hour rate

A full description of each performance indicator can be found in Annex B. The data we select from the PERFORMA database concords with the type of data examined in past attempts that address the NP allocation problem. Most of the previous work focused on A_o as the main object to connect with NP spending. In this study, we have broadened the scope but maintained the original flavour of previous work by examining only high level data. The larger scope of the data will help us discover possible indirect relationships between NP spending and A_o .

We obtained the financial data from FMAS broken down by spares and R&O. The data covers the same time frame (in monthly form) as the performance indicator data. The financial data are placed inside a 13 month year to account for spending invoiced at the end of one fiscal year but expensed in the following fiscal year. We correct for the 13 month year by placing the data from the 13th month into the first month of the new fiscal year. We understand that from an accounting perspective the 13th month represents a separate entity to capture actual previous fiscal year spending relationships, but for our study, we need to treat spending as a continuous process. Moving the 13th month spending into the first fiscal month of the following year has the effect of removing the artificial discontinuous jump that we see in the spending data at fiscal year changes. Since we desire a relationship between incremental changes in the data, we must ensure that we make appropriate comparisons with continuous time. We treat spending on spares, spending on R&O, and total NP spending separately in the analysis.

3.2 Analysis

We break the analysis down into two parts: performance indicators with total NP spending, and performance indicators with spares spending and R&O spending. Before we apply the models of the previous section, we need to put the data in a standard form. Since we are

interested in correlations among changes in the time series, we first recast each time series, $S_j(t)$, as

$$\tilde{\xi}_j(t_i) = \frac{S_j(t_{i+1}) - S_j(t_i)}{S_j(t_i)}. \quad (17)$$

The $\tilde{\xi}_j(t)$ time series represent the percent changes of the original time series. Renormalizing each time series by placing the data in standard form, we have

$$\xi_j(t) = \frac{1}{\sigma_j}(\tilde{\xi}_j(t) - E(\tilde{\xi}_j(t))), \quad (18)$$

which implies that each $\xi_j(t)$ has zero mean and unit variance. Notice that the differenced time series $\tilde{\xi}_j(t)$ contains one less measurement than the original time series. Constructing the time series matrix

$$\mathbf{M}_{ji} = \xi_j(t_i), \quad (19)$$

we find that the normalized correlation matrix becomes,

$$\mathbf{C} = \mathbf{M}\mathbf{M}^T. \quad (20)$$

We use the mathematical structure of eq.(17) through eq.(20) for the time series analysis in the remainder of the paper. By examining the time series data using percent changes, we immediately see that the correlation estimates will yield insight into the elasticity of NP spending on performance.

3.3 Total NP analysis with synchronous time series

For the first part of the analysis, we focus on the performance indicators synchronously matched with total NP spending. In total, we have 14 time series each with 119 measurements. To find information content buried in the correlation matrix, we compute the eigenvalue spectrum and compare the result to the $Q = 119/14$ infinite dimensional random matrix.

Figure 5 shows the result of the decomposition. Notice that the empirical eigenvalue spectrum does not match the expectation from random matrix theory. The $Q = 119/14$ random matrix yields the maximum and minimum eigenvalues of

$$\lambda_{\max} = 1.80 \quad \lambda_{\min} = 0.43, \quad (21)$$

and we see that we have an excess of small and large eigenvalues. While finite size effects and departures from normality in the incremental changes distort the eigenvalue spectrum, the size of the distortions that we see points to the presence of correlated sectors inside the system. In particular, the excess of small eigenvalues suggests the existence of clusters that contain a small number of highly correlated time series in addition to at least one large sector.

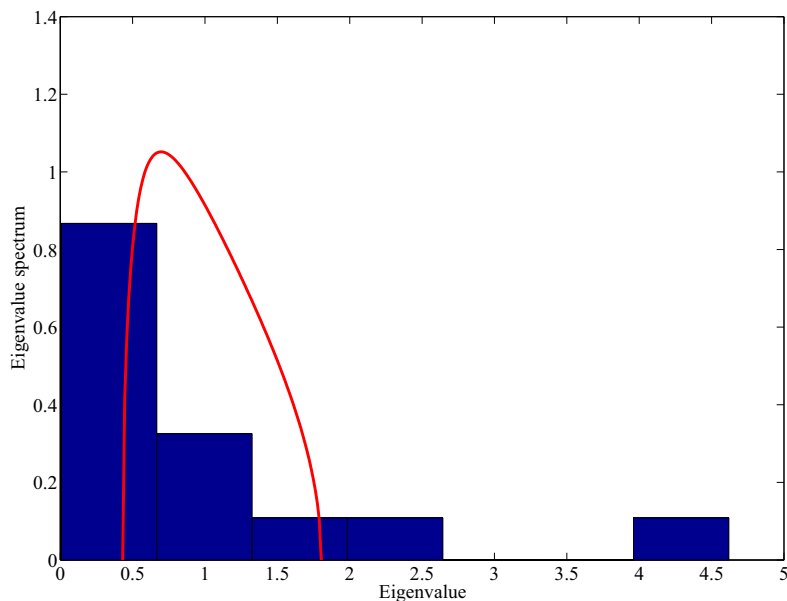


Figure 5: The empirical eigenvalue spectrum (histogram) for total NP spending synchronously matched to performance indicators. The theoretical curve for $Q = 119/14$ infinite random matrix is superimposed.

Using the Kruskal algorithm, we construct the MST for the correlations. Given that we are searching for relationships with either positive or negative correlations, we take the absolute value of the correlations in constructing the MST. Thus, if NP spending negatively correlates with a performance measure, we will interpret that performance measure as being close to NP spending in the ultrametric space. Using the absolute value of the correlations allow us to identify time series that *know about each other* regardless of the type of relationship.

In figure 6, we see that the dendrogram indicates a high level of correlation between *First level* A_o (4) and A_o (2). We also see that eight time series associated with maintenance activities form a larger block inside the data and that *On aircraft maintenance person-hour rate* (10) and *Preventive maintenance person-hour rate* (13) form a tight subgroup. From a qualitative perspective, the clustering we see in the performance measures makes sense. We expect to see a high level of correlation between different A_o measures as well as between certain types of maintenance activities. In building the dendrogram, we used 85% of the maximum ultrametric distance as a cutoff for isolating sectors and the results concord with the distortions we observe in the eigenvalue spectrum relative to expectations from random matrix theory.⁷

⁷The results of this study are not sensitive to changes in the cutoff. NP only begins to cluster if we use

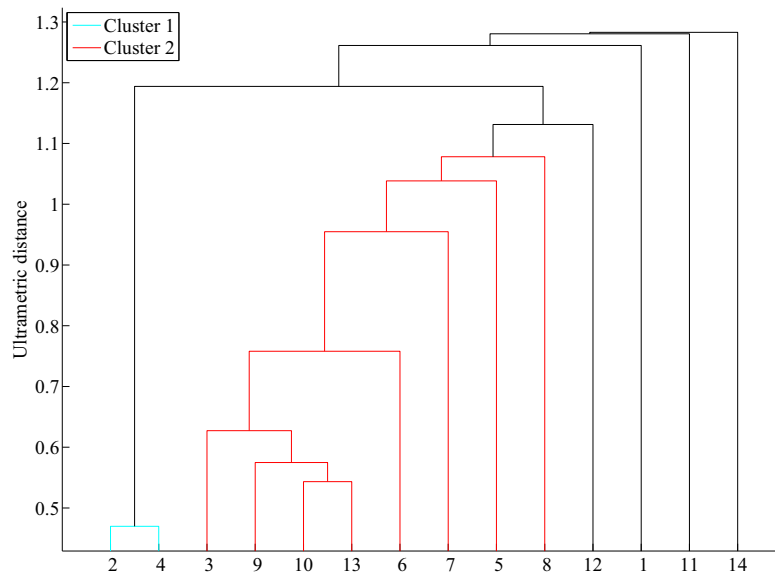


Figure 6: Dendrogram for NP spending (time series 14) synchronously matched to performance indicators. Notice that NP spending branches early in the dendrogram indicating that NP spending lies far from the performance indicators in the ultrametric space. The number labelling for each time series is the same as that given in the text.

The extraction of the precise number of sectors in the data does not represent the central problem of the exercise. The observation that the NP spending time series (series 14) branches out early from the dendrogram in figure 6 forms the central lesson – **NP spending does not form a hub in the MST, nor does NP spending correlate strongly with any of the performance indicators.** Given that ultrametrically NP spending lies far from the performance data clusters, it will be exceedingly difficult to construct a model that evolves NP spending synchronously with performance data.

3.4 Total NP analysis with time lags time

By relaxing the synchronicity condition, we can search for NP spending clustering in the presence of time lags. Given that spending on equipment often produces benefits at a later date (after all, maintenance and improvements take time), we must search for clustering without the use of synchronous time series. Specifically, since NP spending represents the key time series in the analysis, we consider lags of up to one year in the NP spending rela-

95%+ of the maximum ultrametric distance. Clusters with cutoff at the 95% level can be explained by noise alone.

tive to the performance measures. Lags in NP spending will identify temporal relationships between NP allocation and the performance of the fleet.

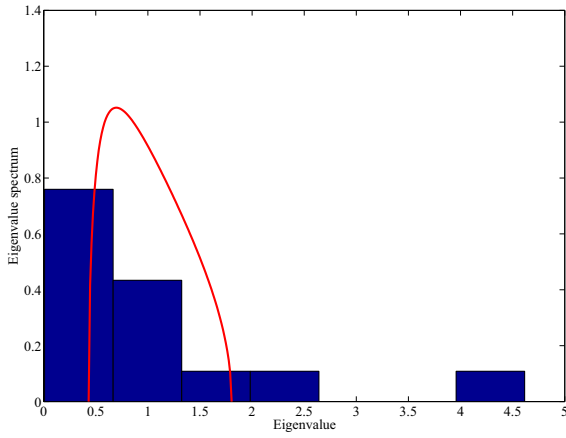
Figure 7 shows the eigenvalue spectrum for time lags of 1 month, 2 months, 3 months, 6 months and 1 year. In each case we see an excess of large and small eigenvalues which suggests the presence of data clustering. We know from the synchronous analysis that some of these clusters represent the original synchronous performance measure clusters. The dendrogram for each time lag scenario, shown in figure 8, demonstrates that NP does not form a cluster with any of the performance measures. We see that NP spending branches out early in each dendrogram which tells us that **even in the presence of time lags, NP spending does not significantly correlate with any performance measure**. Again, the analysis suggests that model building with NP spending and performance data will prove extraordinarily challenging.

3.5 Spares and R&O analysis with synchronous time series

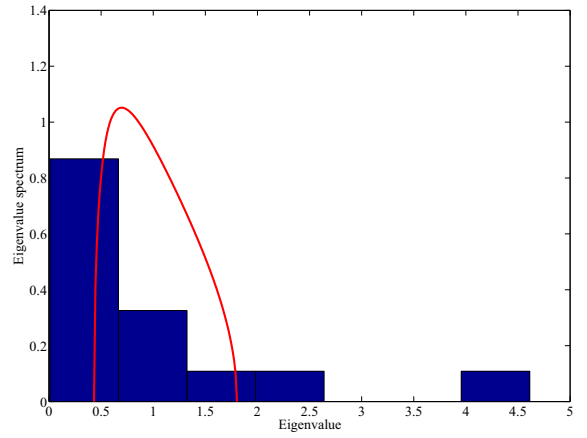
We repeat the analysis for spares and R&O treated as individual time series. In this case, we have 15 time series in which the last two time series (14 and 15 respectively) represent spares and R&O spending while the remaining 13 time series represent the original performance indicators. In figure 9 we see the eigenvalue spectrum with no lag in spending along with the corresponding dendrogram. Note that, again, we see an excess of large and small eigenvalues relative to the predictions from random matrix theory. In the corresponding dendrogram we see that the performance indicators account for the clustering and, as in the total NP spending analysis, spares and R&O spending do not form a central hub or network within the time series set.

3.6 Spares and R&O analysis with time lags

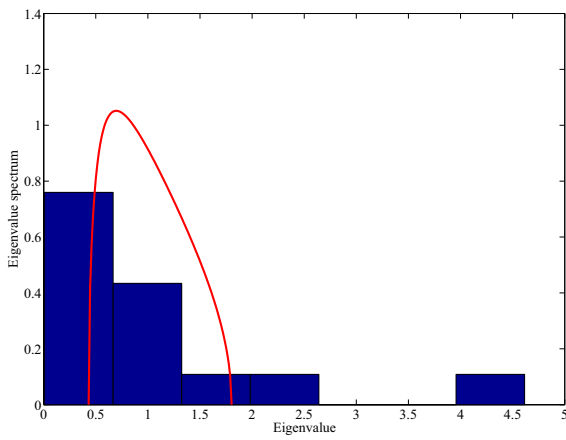
The panels in figure 10 show the empirical eigenvalue spectrum for lagged spares and R&O spending. Again, we see an excess of small and large eigenvalues which suggests the presence of correlated clusters. The dendrograms of figure 11 show that the clusters do not involve the spending time series. The original correlated clusters remain, while spending on spare and R&O continue to branch out early in each dendrogram. These results suggest that using the elasticity for NP spending on spares and R&O as parameter inputs for performance modelling will prove most challenging.



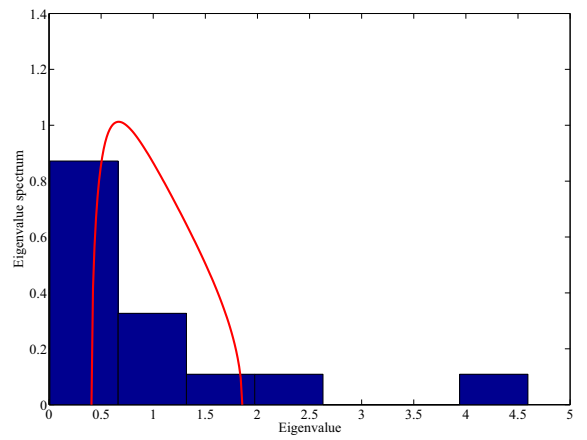
(a)



(b)

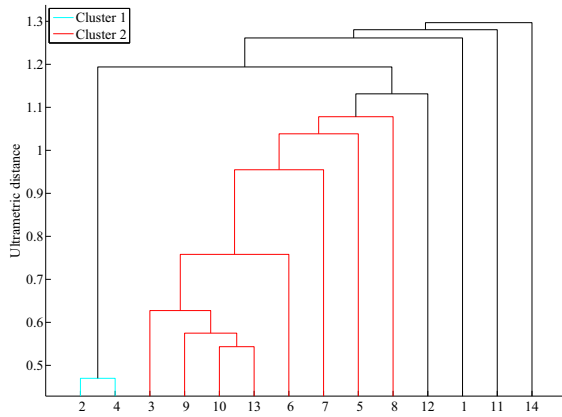


(c)

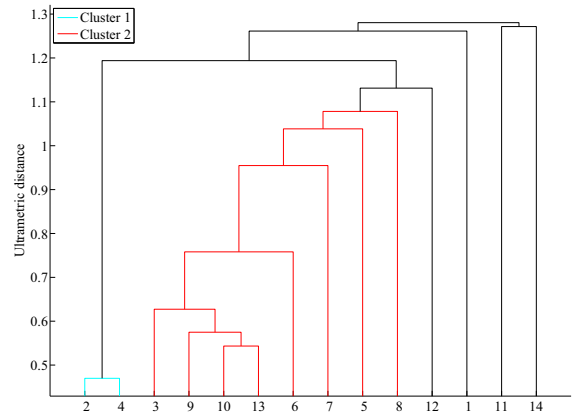


(d)

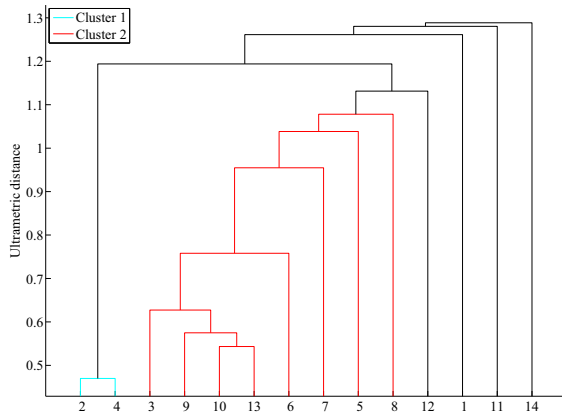
Figure 7: Eigenvalue spectrum of performance indicators with lagged NP spending with theoretical curve (a) lag 1 month, (b) lag 3 months, (c) lag 6 months, and (d) lag 12 months.



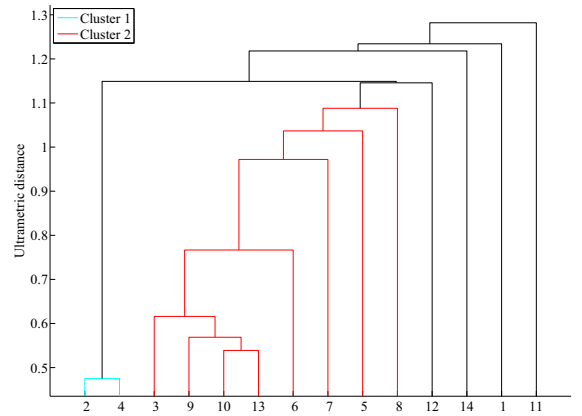
(a)



(b)



(c)



(d)

Figure 8: Dendrogram of performance indicators with lagged NP spending (a) lag 1 month, (b) lag 3 months, (b) lag 6 months, and (b) lag 12 months. Note that NP spending (time series 14) branches early in each dendrogram indicating that NP spending does not form a hub within the MST.

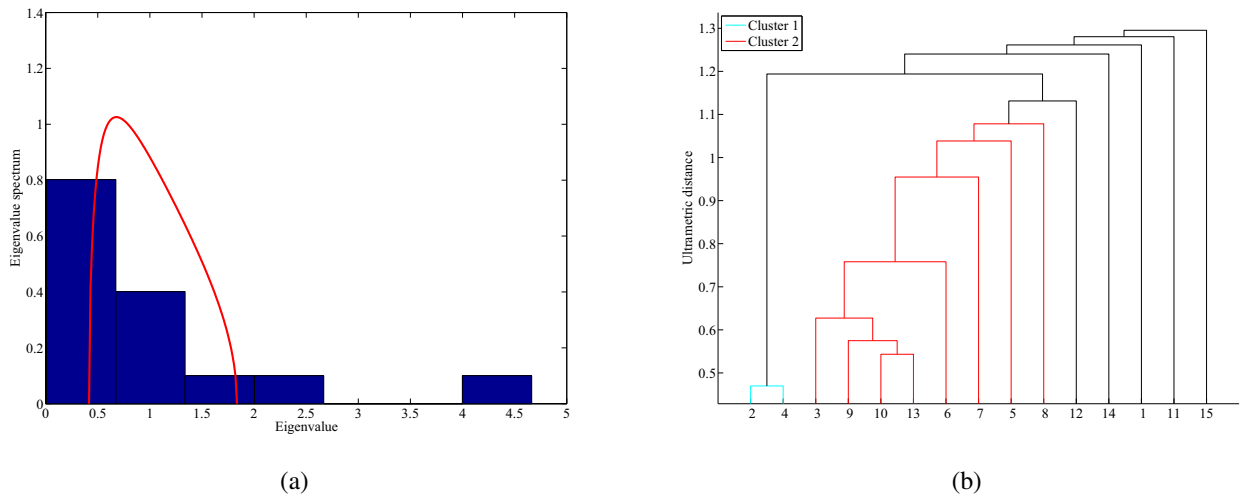
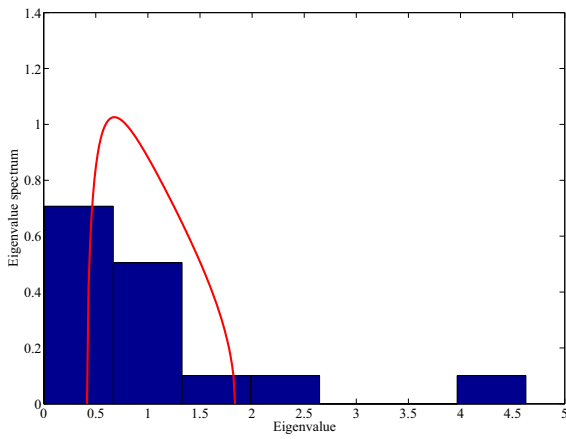


Figure 9: (a) Eigenvalue spectrum with spares and R&O spending synchronously matched with theoretical curve. (b) Dendrogram for the performance indicators with synchronously matched spares and R&O spending (time series 14 and 15).

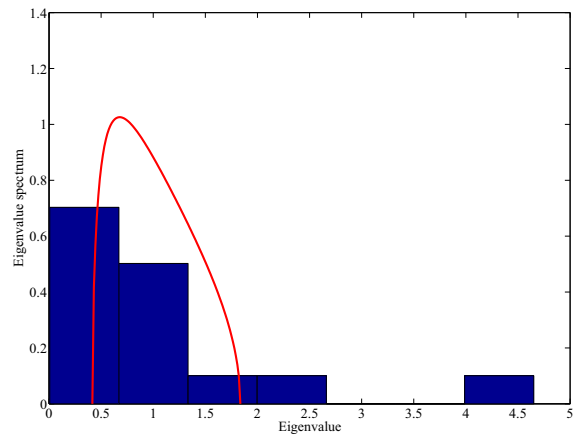
4 Conclusions

Searching for a connection between NP spending and fleet performance indicators represents a difficult problem. Past attempts, which used an assortment of approaches based generally on filter methods, have been met with frustration. In each attempt, an underlying functional relationship was assumed. The essential idea of each method centered on statistically extracting an elasticity parameter between spending and performance. As a minimum, any model connecting fleet performance to NP spending requires an understanding of the level of correlation between relevant time series. Using random matrix theory and the concept of an ultrametric space, we find that the frustrations of past attempts stem from the high level of noise dressing in the correlation matrix. While it is eminently reasonable to expect an elasticity relationship between NP spending and performance, the correlation matrix refuses to shed light on this problem and therefore stymies model construction for a better articulation between spending and performance.

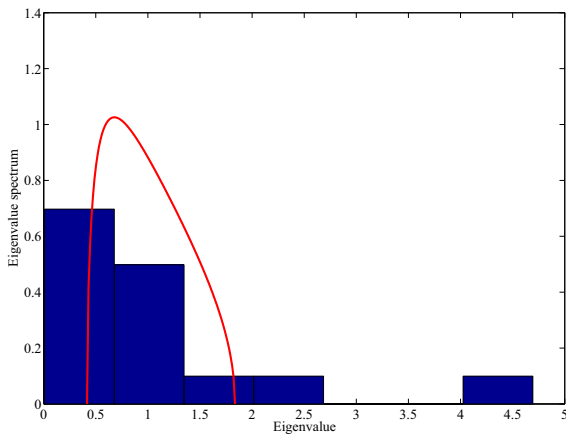
The application of our techniques to the CC130 have demonstrated that noise dressing represents a serious obstacle in developing a model that would connect NP spending to fleet performance. In some sense, we should not be surprised by our results. NP spending connects to the larger economy with many exogenous factors. Given that fluctuations in the economy influence the costs associated with the CC130 fleet, performance can quickly divorce from underlying financials. An attempt to build a multiple regression model or a filter model that uses economic variables in addition to fleet performance would almost certainly become an unwieldy ad hoc construction. The noise dressing in the correlation



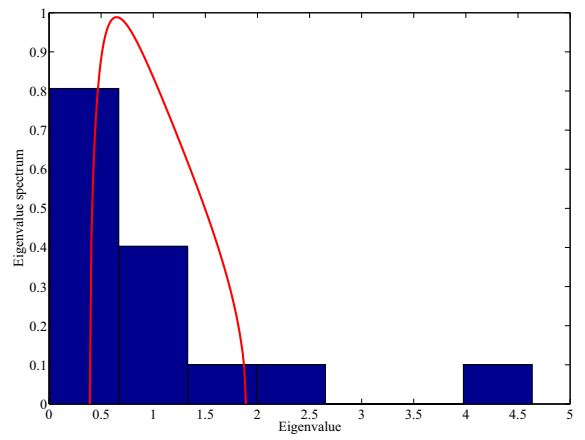
(a)



(b)

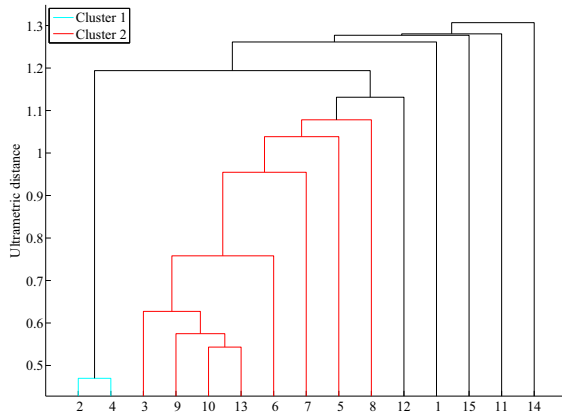


(c)

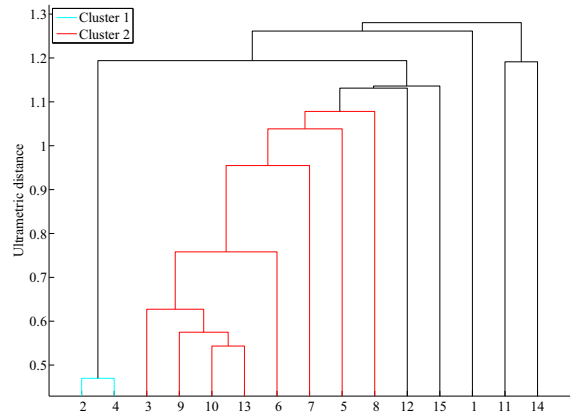


(d)

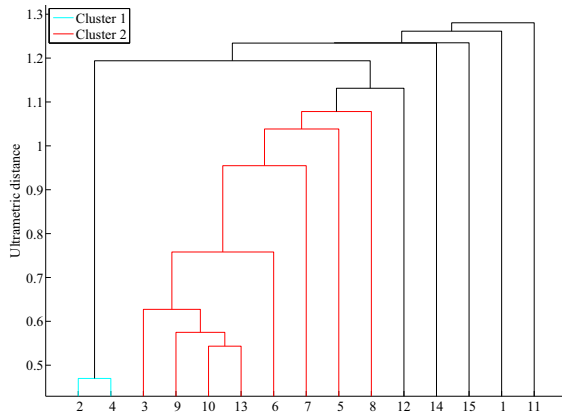
Figure 10: Eigenvalue spectrum of performance indicators with lagged spares and R&O spending with theoretical curve (a) lag 1 month, (b) lag 3 months, (b) lag 6 months, and (b) lag 12 months.



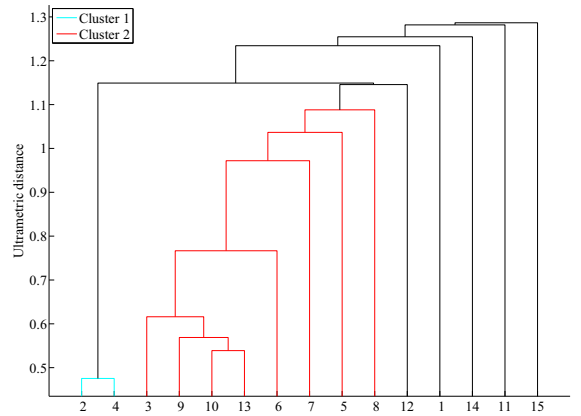
(a)



(b)



(c)



(d)

Figure 11: Dendrogram of performance indicators with lagged NP spending (a) lag 1 month, (b) lag 3 months, (b) lag 6 months, and (b) lag 12 months. Note that spares and R&O spending (time series 14 and 15) branch early in each dendrogram indicating that spares and R&O spending do not form a hub within the MST.

matrix tells us that randomness plays a large role in the correlation between NP spending and fleet performance.

We should understand that our results paint a positive picture of the CC130 fleet. Changes in NP spending at the levels observed in the data have little impact on performance. Broadly, we can conclude that the maintenance activity is highly robust – spending shocks of the size observed in the data do not have a statistical impact on major performance indicators⁸. While we do not see a correlation between performance and NP spending, clearly if the NP spending level is lowered sufficiently, we will eventually begin to see correlations above the noise dressing as the fleet begins to starve. At some critical spending level, the fleet would not be serviceable and spending would correlate strongly with the ability to bring individual aircraft online. In this sense, we expect that the elasticity of the fleet with respect to spending will go through a phase transition at a sufficiently low level of funding support. The results of this paper show that over the ten year history from December 1998 to November 2008, the critical spending level has not been breached.

While we cannot connect spending to performance indicators, we can construct a useful model of A_o . In [14], and [15] it was shown that mean reverting stochastic process capture fleet-wide A_o and an inspection of the CC130 data suggest that such models apply in this case. In previous attempts, the analysts suggested that the best predictor of the A_o is the current A_o value and that the ability to predict A_o separated itself from spending issues [1]. The stochastic mean reverting models add to the picture by demonstrating that A_o in many military fleets have a slow mean reverting factor which gives us a deeper understanding of the fluctuations involved. If ADM(Mat) desires a model that simply forecasts A_o , without costing inputs, the DMGOR can construct robust models.

The methods we use in this paper can be applied to other fleets and equipment. In addition to searching for relationships between spending and performance, we can apply the theory of random matrices to other instances where we need to examine correlations in data. By examining the eigenvalue spectrum and comparing the results with expectations from random matrix theory, we can isolate the effects of correlated sectors – both large and small – in the data. We also avoid ascribing spurious correlations to relationships that do not exist. In the end, the application of random matrix theory with the concept of an ultrametric space for constructing the MST will help us prevent identifying skim milk as cream.

⁸In economic parlance, the response between spending and performance is said to be inelastic.

References

- [1] Dr. P. E. Desmier , Private communication, (February 1, 2009).
- [2] Peter S. Maybeck, Stochastic models, estimation, and control, **Vol** 1,2,& 3, mathematics in Science and Engineering, (1982).
- [3] Robert T. Stengel, Optimal control and estimation, Dover Publications, (1994).
- [4] K. F. Ready, Private communication, (February 06, 2003).
- [5] InnoVision Consulting Inc., AEPM PERFORMA, DV6000.4000.6052.
- [6] Financial Managerial Accounting System,
http://fmas-scfg.mil.ca/top_content/help_desk/index_e.asp?user_language=0.
- [7] Siegmund Brandt, Data Analysis, 3rd Ed., Springer, (1998).
- [8] L. Giada, and M. Marsili, Data clustering and noise undressing of correlation matrices, *Phys. Rev. E* 63, 061101 (2001), [arXiv:cond-mat/0101237], (2001).
- [9] O. Bohigas, and M. J. Giannoni, Random matrix theory and applications, Mathematical and computational methods in nuclear physics, Lecture Notes in Physics **Vol.** 209, Springer-Verlag, New York (1983).
- [10] J.-P. Bouchaud, and M. Potter, Theory of Financial Risk and Derivative Pricing, 2nd Ed., Cambridge University Press (2009).
- [11] V. Plerou, P. Gopikrishnan, B. Rosenow, L. A. Nunes Amaral, Thomas Guhr, and H. E. Stanley, Random matrix approach to cross correlations in financial data, *Phys. Rev. E* 65, 066126 (2002), (2002).
- [12] G. Bonanno, G. Caldarelli, F. Lillo, S. Micciché, N. Vandewalle, and R. N. Mantegna, Networks of equities in financial markets, *Eur Phys J B*, 38, 363-371, (2004), [arXiv:cond-mat/0401300v1], (2004).
- [13] R. N. Mantegna, and H. E. Stanley, An introduction to econophysics, Cambridge University Press, (2007).
- [14] D.W. Maybury, Mean reverting stochastic processes with application, DRDC CORA TN 2009-008, (September 2009).
- [15] D.W. Maybury, Optimal replacement of the CH149 Cormorant fleet, DRDC CORA TM 2009-061, (December 2009).
- [16] D. J. C. MacKay, Information Theory, Inference, and Learning Algorithms, Cambridge University Press, (2007).

Annex A: Random matrix theory primer

In section 2, we learned that we could write the eigenvalue spectrum of a matrix as

$$\rho(\lambda) = \lim_{\varepsilon \rightarrow 0} \frac{1}{M\pi} \text{Im}(\text{Tr} \mathbf{G}(\lambda - i\varepsilon)). \quad (\text{A.1})$$

In deriving eq.(A.1), we required the identity,

$$\frac{1}{x - i\varepsilon} = \text{PP} \frac{1}{x} + i\pi\delta(x) \quad (\varepsilon \rightarrow 0). \quad (\text{A.2})$$

To see that the identity in eq.(A.1) holds, observe that

$$\lim_{\varepsilon \rightarrow 0} \int_{-\infty}^{\infty} \frac{dx}{x - i\varepsilon} = \lim_{\varepsilon \rightarrow 0} \int_{-\infty}^{\infty} \frac{x + i\varepsilon}{x^2 + \varepsilon^2} dx = \lim_{\varepsilon \rightarrow 0} i\varepsilon \int_{-\infty}^{\infty} \frac{1}{x^2 + \varepsilon^2} dx + \lim_{\varepsilon \rightarrow 0} \int_{-\infty}^{\infty} \frac{x}{x^2 + \varepsilon^2} dx. \quad (\text{A.3})$$

We recognize that the integrand of the first integral on the far right-hand side of eq.(A.3) has the form

$$\lim_{\varepsilon \rightarrow 0} \frac{\varepsilon}{\pi(x^2 + \varepsilon^2)} = \delta(x) \quad (\text{A.4})$$

where we have used a distributional identity for the delta function, and we see that the second integral of eq.(A.3) recovers the principal part of the integral of $1/x$. Thus, we have the identity eq.(A.2).

We are left with the task of computing $\text{Tr} \mathbf{G}(\lambda)$. We follow [10] in showing the calculational method. To begin, recognize that we can write the trace over $\mathbf{G}(\lambda)$ as,

$$\text{Tr} \mathbf{G}(\lambda) = \sum_a^N \frac{1}{\lambda - \lambda_a} = \frac{\partial}{\partial \lambda} \log \prod_a^N (\lambda - \lambda_a) = \frac{\partial}{\partial \lambda} \det(\lambda \mathbf{I} - \mathbf{C}) \equiv \frac{\partial}{\partial \lambda} Z(\lambda) \quad (\text{A.5})$$

Since we can write the the determinant of a real symmetric matrix, \mathbf{A} , as an integral,

$$[\det \mathbf{A}]^{-1/2} = \left(\frac{1}{\sqrt{2\pi}} \right)^M \int \exp \left(-\frac{1}{2} \sum_{i,j=1}^M \varphi_i \varphi_j A_{ij} \right) \prod_{i=1}^M d\varphi_i \quad (\text{A.6})$$

and since $\mathbf{C} = \mathbf{H}\mathbf{H}^T$ (\mathbf{H} is an $M \times N$ matrix), we can re-express $Z(\lambda)$,

$$Z(\lambda) = -2 \log \int \exp \left(-\frac{\lambda}{2} \sum_{i=1}^M \varphi_i^2 + \frac{1}{2} \sum_{i,j=1}^M \sum_{k=1}^N \varphi_i \varphi_j H_{ik} H_{jk} \right) \prod_{i=1}^M \left(\frac{d\varphi_i}{\sqrt{2\pi}} \right). \quad (\text{A.7})$$

Instead of using a specific realization of \mathbf{H} , we can compute with its ensemble average. It is not trivial that we can proceed with the ensemble average as we are implicitly assuming that in the large N limit we can substitute the average over the logarithm for the logarithm

of the average. Generally, we cannot make this substitution, but in this case the result stands (in the large N limit) from the replica trick used in condensed matter physics.⁹ To proceed, we imagine that the elements of H are Gaussian *i.i.d.* noise with mean zero and variance σ^2/N . In this case, we find

$$\mathbb{E} \left[\exp \left(\frac{1}{2} \sum_{i,j=1}^M \sum_{k=1}^N \varphi_i \varphi_j H_{ik} H_{jk} \right) \right] = \left(1 - \frac{\sigma^2}{N} \sum_{i=1}^M \varphi_i^2 \right)^{-N/2}. \quad (\text{A.8})$$

We can re-write the expression for the expectation using an integral representation of the delta function with $q = \sigma^2 \sum_{i=1}^M \varphi_i^2$,

$$\delta \left(q - \sigma^2 \sum_{i=1}^M \frac{\varphi_i^2}{N} \right) = \int \frac{1}{2\pi} \exp \left(i\tau \left(q - \sigma^2 \sum_{i=1}^M \frac{\varphi_i^2}{N} \right) \right) d\tau \quad (\text{A.9})$$

which allows us to write,

$$Z(\lambda) = -2 \log \frac{1}{2\pi} \int \int \int \exp \left(-\frac{\lambda}{2} \varphi^2 \right) (1-q)^{-\frac{N}{2}} \exp \left(i\tau \left(q - \sigma^2 \sum_{i=1}^M \frac{\varphi_i^2}{N} \right) \right) dq d\tau \prod_{i=1}^M \left(\frac{d\varphi_i}{\sqrt{2\pi}} \right). \quad (\text{A.10})$$

Making the substitution $z = -2i\tau/N$ we can recast $Z(\lambda)$ as,

$$Z(\lambda) = -2 \log \frac{Ni}{4\pi} \int_{-i\infty}^{i\infty} \int_{-\infty}^{\infty} \exp \left(-\frac{M}{2} (\log(\lambda - \sigma^2 z) + Q \log(1-q) + Qqz) \right) dq dz \quad (\text{A.11})$$

where $Q = N/M$. Using the saddle point method (also known as Laplace's Method, see [16]),

$$\int_a^b \exp(Mf(x)) dx = \sqrt{\frac{2\pi}{M|f''(x_0)|}} \exp(Mf(x_0)) \quad (M \rightarrow \infty), \quad (\text{A.12})$$

where x_0 is the saddle point, we can find that

$$Qq = \frac{\sigma^2}{\lambda - \sigma^2 z} \quad z = \frac{1}{1-q} \quad (\text{A.13})$$

which has the solution

$$q(\lambda) = \frac{\sigma^2(1-Q) + Q\lambda \pm \sqrt{(\sigma^2(1-Q) + Q\lambda)^2 - 4\sigma^2 Q\lambda}}{2Q\lambda}. \quad (\text{A.14})$$

We can now readily find $\mathbf{G}(\lambda)$ by differentiating $Z(\lambda)$, which yields

$$\mathbf{G}(\lambda) = \frac{MQq(\lambda)}{\sigma^2}. \quad (\text{A.15})$$

⁹The general idea is to replicate the system by using m products of the system. Once the replicated system is averaged over the m products, the limit $m \rightarrow 0$ is taken to reveal the result.

Using the imaginary part of $\mathbf{G}(\lambda)$, we find that eq.(A.1), the density of the eigenvalues, becomes,

$$\rho(\lambda) = \frac{\sqrt{4\sigma^2 Q\lambda - (\sigma^2(1-Q) + Q\lambda)^2}}{2\pi\lambda\sigma^2}. \quad (\text{A.16})$$

Note that eq.(A.16) has a maximum and a minimum in the spectrum, namely,

$$\lambda_{\min}^{\max} = \sigma^2 \left(1 + \frac{1}{Q} \pm 2\sqrt{\frac{1}{Q}} \right). \quad (\text{A.17})$$

Thus, random matrix theory predicts that we should see all the eigenvalues contained within the range $[\lambda_{\min}, \lambda_{\max}]$ and distributed according to the spectrum given in eq.(A.16). Figure A.1 shows the spectra, $\rho(\lambda)$, for $Q = 1, 2, 5$.

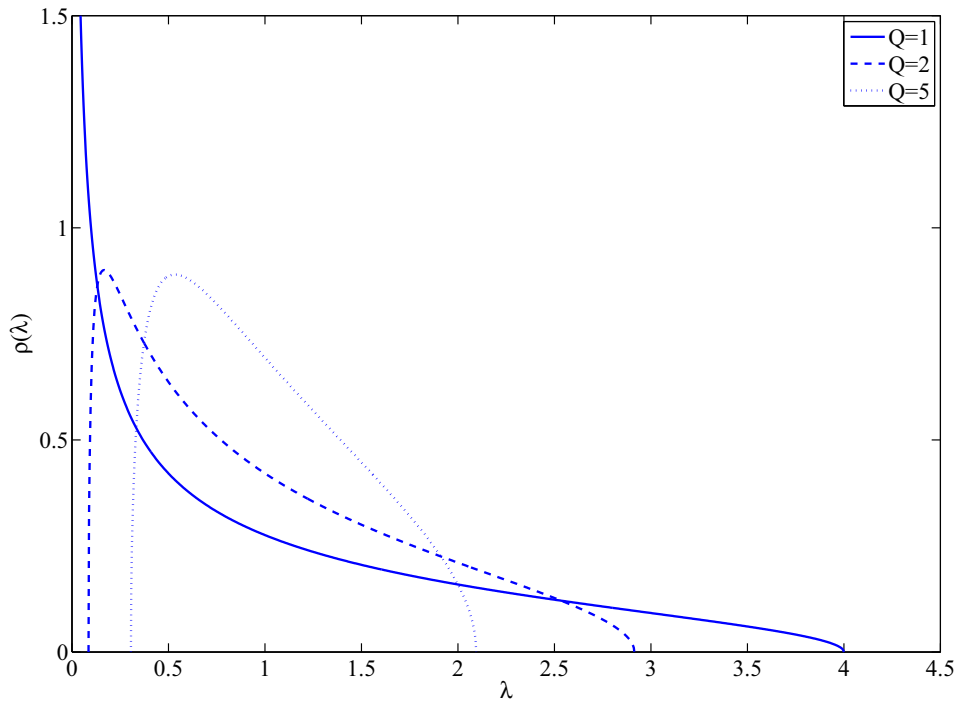


Figure A.1: Eigenvalue spectra for infinite random matrices with $Q = 1, Q = 2, Q = 5$. Note the presence of λ_{\min} and λ_{\max} in each case.

This page intentionally left blank.

Annex B: Fleet indicator definitions

This Annex contains the definitions of the fleet indicators used in the analysis provided in this paper. The definitions listed below are taken verbatim from the PERFORMA database. Further technical information can be found in the PERFORMA database[5].

All Failures

Definition: All Failures are the sum of the On-A/C Failures and the Off-A/C Failures.

- On-A/C Failures: Total number of failures recorded on a CF 349 form against a piece of equipment installed on an Aircraft. Those are determined from all entries recorded on the On-A/C CF 349 maintenance forms against any valid WUC, where the equipment had to be replaced or repaired in order to return the Aircraft to a serviceable status. This includes all valid Sequence 1 and 2 line entries.
- Off-A/C Failures: Total number of failures recorded against uninstalled equipment. An Off-A/C form is defined as a CF 349 form without an Aircraft number or a CF 543 form. A failure will have a Fix = 3 or for non-serialized items, the Fix = 6 with a contractor Fixer Unit Code (3 letters) and a supplementary data of TLRO/TLIR/TLM.

Ao – Operational Availability as % of time

Definition: (Ao) Operational Availability as % of time is the proportion of observed time that a group of Aircraft is in an operable state (not undergoing maintenance) in relation to the total operational time available during a stated period. Operational Availability as percentage of time is calculated using: $Ao = \text{Up Time} / (\text{Up Time} + \text{Down Time})$ Where: “Up Time” is the total actual number of calendar hours where the selected Aircraft are not undergoing any maintenance action during the chosen period (no open CF 349) and the Allocation Code is not “LX”. And: “Up Time + Down Time” is the total number of calendar hours included in the selected period of the analysis. In calculating all downtimes and uptimes, the date and time are translated to the nearest hour based on 24/7 operations.

Corrective Maintenance Person-Hours Rate

Definition: Total number of “Maintenance Person-Hours” reported on CF 349 and CF 543 corrective maintenance forms for every 1000 hours flown by a specific fleet. This calculation involves three defaults when examining MPHRs for a particular component.

- Installation Factor (IF): Quantity of the same item that is installed on a single Aircraft (e.g. there are two engines on the Aircraft). The Installation Factor information is not available so 1 is used as default.

- Fitment Factor (FF): Proportion of a fleet onto which equipment is fitted (e.g. EW equipment is not installed on all Aircraft). The FF information is not available so 1 is used as default (for 100% of fleet).
- Duty Cycle (DC): Proportion of time a piece of equipment is on when an Aircraft is operating (e.g. even when installed, EW equipment does not operate for the entire duration of a flight). The DC information is not available so 1 is used as default (for 100% of mission time).

First Level Availability

Definition: First Level Availability (First Level Ao) is the proportion of observed time where routine maintenance is not carried out on the group of “First Level Aircraft” (First Level Up Time), in relation to the total cumulative time where those Aircraft could have been available (First Level Total Time). The First Level Availability is based on the time that an aircraft is considered to be in First Level and not on calendar time. Therefore, an aircraft may be in First Level for only two days in one month and have First Level Availability of 80% for that month if it was available for 80% of the time that it was in First Level. First Level Availability is an availability calculation done specifically for the group of “First Level Aircraft” which are those that are considered to be used for the daily flying; they are owned by military units, have an allocation code “CX” or “GX” and can either be serviceable or be undergoing “First Level maintenance”, generally 1st level of maintenance. First Level Availability is calculated using: $\text{First Level Ao} = (\text{First Level Uptime}) / (\text{First Level Total Time})$ Where: The “First Level Total Time” is calculated using: $\text{First Level Total Time} = (\text{First Level Uptime} + \text{First Level Downtime})$

Note that the First Level Total Time is not necessarily the complete calendar time for the query expression but the calendar time during which an aircraft was considered to be in first level. The downtimes excluded from the “First Level Total Time” calculation are the downtimes for a distinct tail number where the CF 349s reporting On-A/C maintenance work are from one of the following categories:

- “Non-routine maintenance” action (see list below);
- ”Routine maintenance” (see list below) occurring simultaneously with a non-routine; maintenance action (i.e. put u/s date of the "routine maintenance" is during a “non-routine maintenance” form downtime);
- Maintenance action reported by 2nd or 3rd line (i.e. How Found = D); and
- Maintenance action reported by a non-military fixer unit (i.e. alphanumeric fixer unit)

The “First Level Downtime” is calculated from the downing events for a distinct tail number where the CF 349s reporting On-A/C maintenance work are not from the four categories

listed above. The downtimes for all these downing events are calculated for each distinct tail number and added up to get the total “First Level Downtime”. A downing event downtime is composed of a single or a group of CF 349s reporting work performed On-A/C (i.e. CF 349s must have a tail number) from the time the Aircraft was first put u/s to the completion of the maintenance work that brings the Aircraft to a serviceable status. The downtime calculation for any downing event starts when a CF 349 form is opened against a distinct tail number (put u/s date-time when the Aircraft becomes unserviceable) and ends when the last CF 349 is closed ’ (last certified serviceable date-time bringing the Aircraft back to a serviceable status) The “First Level Up Time” is defined as any period where a First Level Aircraft is not undergoing maintenance.

Flying Hours

Definition: Total flying hours recorded by the aircrew during a given time period as reported via the monthly AUSR report.

Mean Flying Time Between On-A/C Corrective Forms

Definition: Average elapsed flying time between two consecutive On-A/C Corrective Forms. This is determined by dividing the total operating hours of a piece of equipment over a given period by the total number of On-A/C Corrective Forms recorded against that equipment. For periods with no forms or events occurring, the operating hours will be shown.

Mean Flying Time Between On-A/C Preventive Forms

Definition: Average elapsed flying time between two consecutive On-A/C Preventive Forms. This is determined by dividing the total operating hours of a piece of equipment over a given period by the total number of On-A/C Preventive Forms recorded against that equipment. For periods with no forms or events occurring, the operating hours will be shown. This parameter is more suitable for analysis at the system or component level.

Mean Flying Time Between Downing Events

Definition: MFTBDE indicates the average flying hours between two consecutive Aircraft Downing Events. A downing event refers to any single occurrence, or group of occurrences, where an Aircraft is brought from a Serviceable/Operational status to an Unserviceable/Repair status. These include both Preventive and Corrective Maintenance Actions reported against an operational Aircraft. Only forms with a numerical fixer unit are included in an event. A downing event may include several failures that are all repaired following the single downing event.

Off-A/C Maintenance Person-Hours Rate

Definition: Total number of “Maintenance Person-Hours” reported on “Off-A/C” forms for every 1000 hours flown by a specific fleet or selected Aircraft.

This calculation involves three defaults when examining MPHRs for a particular component.

- Installation Factor (IF): Quantity of the same item that is installed on a single Aircraft (e.g. there are two engines on the Aircraft). The Installation Factor information is not available so 1 is used as default.
- Fitment Factor (FF): Proportion of a fleet onto which equipment is fitted (e.g. EW equipment is not installed on all Aircraft). The FF information is not available so 1 is used as default (for 100% of fleet).
- Duty Cycle (DC): Proportion of time a piece of equipment is on when an Aircraft is operating (e.g. even when installed, EW equipment does not operate for the entire duration of a flight). The DC information is not available so 1 is used as default (for 100% of mission time).

On-A/C Maintenance Person-Hours Rate

Definition: Total number of “Maintenance Person-Hours” reported on “On-A/C” forms for every 1000 hours flown by a specific fleet or selected Aircraft.

This calculation involves three defaults when examining MPHRs for a particular component.

- Installation Factor (IF): Quantity of the same item that is installed on a single Aircraft (e.g. there are two engines on the Aircraft). The Installation Factor information is not available so 1 is used as default.
- Fitment Factor (FF): Proportion of a fleet onto which equipment is fitted (e.g. EW equipment is not installed on all Aircraft). The FF information is not available so 1 is used as default (for 100% of fleet).
- Duty Cycle (DC): Proportion of time a piece of equipment is on when an Aircraft is operating (e.g. even when installed, EW equipment does not operate for the entire duration of a flight). The DC information is not available so 1 is used as default (for 100% of mission time).

On Aircraft Robs Maintenance Person-Hour Rate

Definition: Number of “Maintenance Person-Hours” reported against a ROB on “On-A/C forms” for every 1000 hours flown by a specific fleet or selected Aircraft. This calculation involves three defaults when examining MPHRs for a particular component.

- Installation Factor (IF): Quantity of the same item that is installed on a single Aircraft (e.g. there are two engines on the Aircraft). The Installation Factor information is not available so 1 is used as default.

- Fitment Factor (FF): Proportion of a fleet onto which equipment is fitted (e.g. EW equipment is not installed on all Aircraft). The FF information is not available so 1 is used as default (for 100% of fleet).
- Duty Cycle (DC): Proportion of time a piece of equipment is on when an Aircraft is operating (e.g. even when installed, EW equipment does not operate for the entire duration of a flight). The DC information is not available so 1 is used as default (for 100% of mission time).

Ops Mission Aborts Rate

Definition: Total number of “Ops Mission Aborts” reported for every 1000 hours flown by a specific fleet.

Rate calculations involve three defaults.

- Installation Factor (IF): Quantity of the same item that is installed on a single Aircraft (e.g. there are two engines on the Aircraft). The Installation Factor information is not available so 1 is used as default.
- Fitment Factor (FF): Proportion of a fleet onto which equipment is fitted (e.g. EW equipment is not installed on all Aircraft). The FF information is not available so 1 is used as default (for 100% of fleet).
- Duty Cycle (DC): Proportion of time a piece of equipment is on when an Aircraft is operating (e.g. even when installed, EW equipment does not operate for the entire duration of a flight). The DC information is not available so 1 is used as default (for 100% of mission time).

Preventive Maintenance Person-Hours Rate

Definition: Total number of “Maintenance Person-Hours” reported on CF 349 and CF 543 preventive maintenance forms for every 1000 hours flown by a specific fleet. This calculation involves three defaults when examining MPHRs for a particular component.

- Installation Factor (IF): Quantity of the same item that is installed on a single Aircraft (e.g. there are two engines on the Aircraft). The Installation Factor information is not available so 1 is used as default.
- Fitment Factor (FF): Proportion of a fleet onto which equipment is fitted (e.g. EW equipment is not installed on all Aircraft). The FF information is not available so 1 is used as default (for 100% of fleet).
- Duty Cycle (DC): Proportion of time a piece of equipment is on when an Aircraft is operating (e.g. even when installed, EW equipment does not operate for the entire duration of a flight). The DC information is not available so 1 is used as default (for 100% of mission time).

List of Acronyms

ADM(Mat)	Assistant Deputy Minister (Materiel)
A _o	Operational Availability
AUSR	Aircraft Utilization Statistical Report
CORA	Centre for Operational Research and Analysis
COS(Mat)	Chief of Staff (Materiel)
DCOS(Mat)	Deputy Chief of Staff (Materiel)
DMGOR	Directorate Materiel Group Operational Research
DND	Department of National Defence
DRDC	Defence Research and Development Canada
FMAS	Financial and Managerial Accounting System
ILS	Integrated Logistics Support
MST	Minimal Spanning Tree
NP	National Procurement
PANACEA	Providing A New Assessment for Costing Equipment Availability
R&O	Repair and Overhaul
TLRO	Third Line Repair and Overhaul
TLIR	Third Line Inspection and Repair
TLM	Third Line Maintenance
WUC	Work Unit Code

Distribution list

DRDC CORA TM 2010-168

Internal distribution

- 6 Author
- 1 DG CORA/DDG CORA/CS/SH(J/C)/(1 Copy on circ)
- 1 DST Air
- 1 Section Head (Air)
- 1 DASOR
- 1 CFAWC ORT
- 1 DRDC CORA Library

Total internal copies: 12

External distribution

Department of National Defence

- 1 COS(Mat)
- 1 DCOS(Mat)
- 1 DGAEPM
- 1 DAEPM(M)

Total external copies: 4

Total copies: 16

This page intentionally left blank.

DOCUMENT CONTROL DATA		
(Security classification of title, body of abstract and indexing annotation must be entered when document is classified)		
<p>1. ORIGINATOR (The name and address of the organization preparing the document. Organizations for whom the document was prepared, e.g. Centre sponsoring a contractor's report, or tasking agency, are entered in section 8.)</p> <p>Defence R&D Canada – CORA Dept. of National Defence, MGen G.R. Pearkes Bldg., 101 Colonel By Drive, Ottawa, Ontario, Canada K1A 0K2</p>	<p>2. SECURITY CLASSIFICATION (Overall security classification of the document including special warning terms if applicable.)</p> <p>UNCLASSIFIED</p>	
<p>3. TITLE (The complete document title as indicated on the title page. Its classification should be indicated by the appropriate abbreviation (S, C or U) in parentheses after the title.)</p> <p>A Random Matrix Theory Approach to National Procurement Spending</p>		
<p>4. AUTHORS (Last name, followed by initials – ranks, titles, etc. not to be used.)</p> <p>Maybury, D.W.</p>		
<p>5. DATE OF PUBLICATION (Month and year of publication of document.)</p> <p>August 2010</p>	<p>6a. NO. OF PAGES (Total containing information. Include Annexes, Appendices, etc.)</p> <p>50</p>	<p>6b. NO. OF REFS (Total cited in document.)</p> <p>16</p>
<p>7. DESCRIPTIVE NOTES (The category of the document, e.g. technical report, technical note or memorandum. If appropriate, enter the type of report, e.g. interim, progress, summary, annual or final. Give the inclusive dates when a specific reporting period is covered.)</p> <p>Technical Memorandum</p>		
<p>8. SPONSORING ACTIVITY (The name of the department project office or laboratory sponsoring the research and development – include address.)</p> <p>Defence R&D Canada – CORA Dept. of National Defence, MGen G.R. Pearkes Bldg., 101 Colonel By Drive, Ottawa, Ontario, Canada K1A 0K2</p>		
<p>9a. PROJECT NO. (The applicable research and development project number under which the document was written. Please specify whether project or grant.)</p> <p>N/A</p>	<p>9b. GRANT OR CONTRACT NO. (If appropriate, the applicable number under which the document was written.)</p>	
<p>10a. ORIGINATOR'S DOCUMENT NUMBER (The official document number by which the document is identified by the originating activity. This number must be unique to this document.)</p> <p>DRDC CORA TM 2010-168</p>	<p>10b. OTHER DOCUMENT NO(s). (Any other numbers which may be assigned this document either by the originator or by the sponsor.)</p>	
<p>11. DOCUMENT AVAILABILITY (Any limitations on further dissemination of the document, other than those imposed by security classification.)</p> <p><input checked="" type="checkbox"/> Unlimited distribution</p> <p><input type="checkbox"/> Defence departments and defence contractors; further distribution only as approved</p> <p><input type="checkbox"/> Defence departments and Canadian defence contractors; further distribution only as approved</p> <p><input type="checkbox"/> Government departments and agencies; further distribution only as approved</p> <p><input type="checkbox"/> Defence departments; further distribution only as approved</p> <p><input type="checkbox"/> Other (please specify):</p>		
<p>12. DOCUMENT ANNOUNCEMENT (Any limitation to the bibliographic announcement of this document. This will normally correspond to the Document Availability (11). However, where further distribution (beyond the audience specified in (11)) is possible, a wider announcement audience may be selected.)</p>		

13. ABSTRACT (A brief and factual summary of the document. It may also appear elsewhere in the body of the document itself. It is highly desirable that the abstract of classified documents be unclassified. Each paragraph of the abstract shall begin with an indication of the security classification of the information in the paragraph (unless the document itself is unclassified) represented as (S), (C), (R), or (U). It is not necessary to include here abstracts in both official languages unless the text is bilingual.)

We apply the methods of random matrix theory to search for relationships between National Procurement spending and the performance of the CC130 fleet. By understanding the eigenvalue spectrum of correlation matrices connected to performance and spending, we construct the minimal spanning tree of the system to identify networked hierarchies in the data. We find that no meaningful relationship exists between spending and high level performance indicators, suggesting that the fleet responds to spending shocks in an inelastic manner. The results indicate that the CC130 fleet is maintained robustly and that funding has not fallen below a critical level that would induce correlations between spending and performance. The techniques we apply in this study can be applied generally to any project that requires an understanding of correlations in data.

14. KEYWORDS, DESCRIPTORS or IDENTIFIERS (Technically meaningful terms or short phrases that characterize a document and could be helpful in cataloguing the document. They should be selected so that no security classification is required. Identifiers, such as equipment model designation, trade name, military project code name, geographic location may also be included. If possible keywords should be selected from a published thesaurus. e.g. Thesaurus of Engineering and Scientific Terms (TEST) and that thesaurus identified. If it is not possible to select indexing terms which are Unclassified, the classification of each should be indicated as with the title.)

Dendrogram
Correlation
Fleet performance
National procurement spending
Minimal spanning tree
Random matrix theory



www.drdc-rddc.gc.ca